COMPARING TWO SYSTEMS FOR DIGITAL PHOTOGRAMMETRY: A METRIC CAMERA & A PHOTOGRAMMETRIC SCANNER VERSUS A SEMIMETRIC CAMERA & A DTP SCANNER

Gianfranco FORLANI
Department of Civil Engineering
University of Parma
Viale delle scienze, 43100 Parma
E-mail: forlani@parma1.eng.unipr.it
ITALY

Livio PINTO
Department of Surveying (DIIAR)
Politecnico of Milan
P.zza L. da Vinci 32, 20133 Milano
E-mail: livio@mail.polimi.it
ITALY

KEY WORDS: LSM, Target Location, Scanner, Accuracy

ABSTRACT

The paper[1] reports on the survey of about 600 targets on a 1 x 1.5 m flat panel, to be used for calibration and orientation of a small resolution trinocular system (accuracy required: 0.1 mm). The survey has been executed with two systems: the first made of a metric camera with a metric scanner, the second made of a semimetric camera and a DTP scanner, in order to compare their performance.
After image digitization at 1200 dpi, the transformation from pixel to photo coordinate system was computed by an affine transformation for the metric images, while for the semimetric images, for each patch of the reseau, a projective transformation was applied, after removing possible gross errors. Likewise, initial target locations for the l.s.m were computed by identifying 4 targets on each image and computing an 8 parameters transformation to their nominal position.
After a preliminary block adjustment of the two set of images, the pattern of the residuals has been analyzed. While for the semimetric cameras the behaviour may be attributed to scanning inaccuracies, locally systematic effects appear in the metric images, whose nature has been investigated. Only the block measured with the metric camera turned out to satisfy the accuracy requirements.

1. INTRODUCTION

The development of high resolution solid state sensors, capable of matching the image format of semimetric cameras, is likely to make soon obsolete any film-based system: analogue image acquisition followed by image scanning cannot compete in the long term with the advantages of flexibility and straightforwardness of an all-digital procedure.
Though not any more in production, metric cameras are still in use while semimetric cameras, still have a (shrinking) market share; people are somehow reluctant to replace them, in the light of years of use and remarkable performance. On the other side, the availability of many software programs for interactive measurement on digital images, either monoscopic or stereoscopic, has greatly widened the diffusion of photogrammetry as a measurement tool among non-photogrammetrists. Therefore, at least in medium and low level accuracies projects, such as in architecture, these kind of systems are often used, taking advantage of low cost DTP image scanners.
In this paper we describe the performance of two such systems in a survey with a target in terms of relative accuracy of about 1:18000 (computed as the required accuracy on the object diveded by object size). The aim of the survey was to provide reference coordinates for a large number of targets, distributed over a nominally flat panel (see figure 1) (flatness better than 1 mm over the whole size, approximately 150x100 cm), to be used for the calibration of a small resolution digital trinocular system. In order to achieve the goal theodolite measurement were soon ruled out, due to the high number of points (several hundreds) and to the fact that the target were homogeneous, lacking any fine detail in the centre, good for the collimation in the short range. It was therefore decided to use photogrammetric techniques. At DIIAR there are not yet digital cameras for metric application, but a metric camera (Wild P31) and a semimetric camera (Rollei 6006) are available. We had some previous experience with DTP scanners and semimetric cameras for similar applications, therefore we decided to take the opportunity to compare the performance of two different systems: the semimetric camera coupled with a DTP scanner and the metric camera coupled with a photogrammetric scanner. The design of the two photogrammetric networks, the image acquisition and the image scanning are described in section 2. Section 3 and 4 discuss the procedure for the determination of the image-to-pixel transformation and the semi-automatic measurement of the reseau and of the targets.

[1] This paper has been presented at the Symp. of ISPRS Comm. V in Hakodate, June 1998

Results of the bundle adjustment for the two sets of image coordinates are presented in section 5, paying attention to the pattern of the residuals, to analyze unmodeled image deformations.

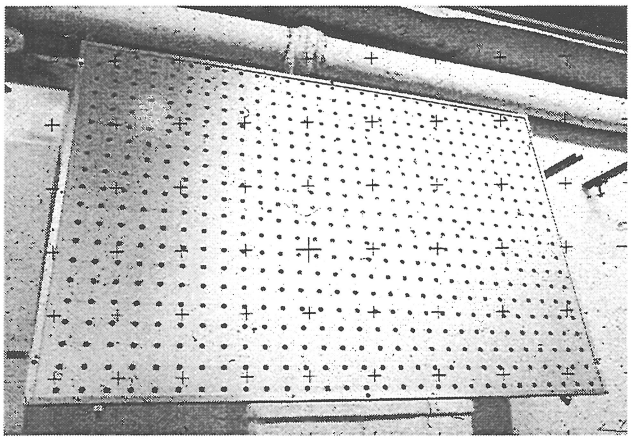

Figure 1 - The surveyed panel (Rollei image).

2. NETWORK DESIGN AND DATA ACQUISITION

The panel has a structure at the same time very rigid and lightweight, thanks to the material used and to the honeycomb assembly. The targets are simply made of black disks, with a diameter of 1.25 cm, regularly arranged in 20 rows and 29 columns (580 overall), 5 cm apart, stuck to the panel. The accuracy required for the XYZ target positions was 0.1 mm. Based on previous experiences (Forlani et al., 1996a), we assumed a measurement accuracy for image (photo) coordinates around 5 micrometers.

The network design, to ensure the reliability necessary to control the results of automatic measurements, was based on a small block made of 4 slightly convergent images and of 4 strongly convergent images, two from the left and two from the right side (see figure 2), with both cameras; the Rollei images are more convergent and have a larger baselenght.

As far as the P31 camera is concerned, we had available a 100 mm lens with additional rings. Given the object size and taking into account the need for convergent stations, we choose a ring ensuring a depth of field from 1.3 to 1.9 m at f/22. Image scale ranges from 1:13 to 1:19. As far as the Rollei camera is concerned, we used a 40 mm lens at f/32 with a stop setting which allows a depth of field from 0.77 to 2.20 m. Image scale ranges from 1:20 to 1:55. Each image covers the whole object.

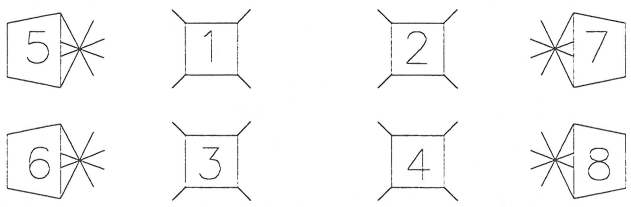

Figure 2 - The photogrammetric network.

Illumination indoor turned out to be a problem, due to the reflectivity of the panel surface and to non optimal lighting equipment, especially for the P31 images, where the matte screen didn't help to position in the best way the lamps: some areas of the panel show therefore much less contrast than others. Eight control points were determined using different targets (6 along the edges and 2 in the middle of the panel) by forward intersection from three stations with a Wild T2000 theodolite; their accuracy turned out to be better than 0.1 mm in all coordinates.

2.1 Film scanning

Image scanning for both set of images was performed directly on the negatives, at the resolution of 1200 dpi (20 μm) under the conservative assumption of a measurement accuracy of about 1/10 of pixel in the digital images. The P31 set was digitized with an Helava DSW 100 (about 24 MB per image), while the Rollei set with an uncalibrated AGFA Horizon (about 7.5 MB per image), in the laboratories of two photogrammetric companies. No local contrast enhancement techniques were applied to the original images, therefore the above mentioned contrast differences are still clearly visible on the images.

3. PIXEL TO IMAGE TRANSFORMATION

The transformation from pixel to image system was computed with a different model for each camera, to try to compensate for scanning deformations in the Rollei images.

In the images of the metric camera, the fiducials were interactively approximately located and their position refined by l.s. template matching. Then an affine tranformation was applied to convert the pixel values to image coordinates. In the images of the semimetric camera five reseau crosses are manually identified and located in each image. The approximate positions of the remaining targets is first predicted by an 8-parameter transformation (rectification) and then refined by l.s. template matching. Rather than using a single affine transformation for the whole image, an 8-parameter transformation is afterwards computed for each group of 4 crosses, in the hope of a better adaptation to local image deformation (Forlani et al., 1996b).

The measurement of some crosses may fail or introduce bias in the measured position because of the image background (see figure 3). To remove possible gross errors, a robust affine transformation is first computed. Then, the position of the crosses where correlation fails are computed based on the position of the neighbouring measured crosses, to complete the reseau and apply the local transformation.

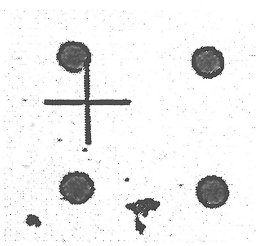

Figure 3 - Interference between crosses and targets.

Out of the total of 40 fiducials, template matching on the P31 images failed to measure 5 crosses with a correlation better than 0.75. The value for σ_0 is bad in two cases (about 10 μm) and the overall result (see Table 1) is not too good in pixel units (perhaps due to disturbances in the background) and exceeds the nominal scanner geometric accuracy. As far as the Rollei is concerned, out of the 121 crosses, 76 were measured on average in each image (basically, almost only those on the panel, since the background is rather dark) with a correlation threshold of 0.8. The number of crosses measured is larger in the less convergent images, thanks to the negligible interference with the targets, which increases with increasing perspective deformations. The average value of σ_0 is twice as much as for the P31, but acceptable given the scanner characteristics. The residuals of the affine transformation do not show a random pattern; their behaviour is roughly the same in all images and is characterized by large row-wise components, typically along a pair of adjacent rows and smaller values elsewhere (see figure 4).

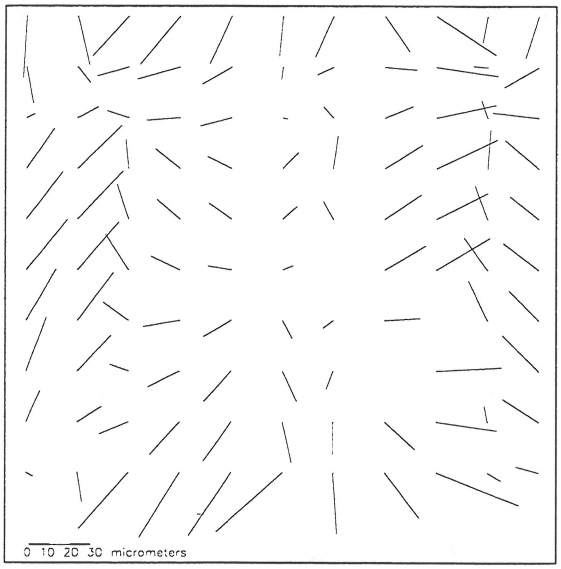

Figure 4 – Residuals of the affine transformation for the reseau.

Since scanning of all the images was performed in the same pass on the Horizon, no clear relationship can be drawn about scanning errors, except for the clear difference in magnitude of the row and column components. Table 1 shows a summary of the transformation for the two sets of images.

	RMS(σ_0) (pix)	RMS(σ_0) (μm)	MAX(σ_0) (pix)	MAX(σ_0) (μm)
P31	0.27	5.4	0.40	8.0
Rollei	0.48	9.7	0.60	12.0

Table 1 - Pixel to image transformation.

4. POINT TRANSFER AND TARGET MEASUREMENT

Thanks to the very simple object structure and with a small amount of interactive work, all target positions were approximately located on each image, basically using the same procedure applied for the reseau cross identification of the semi-metric images described above. First, all targets were labelled and their x, y coordinates automatically assigned, based on their grid-like spacing, in an arbitrary plane reference system. Then, in each image, 5 targets (to check against blunders in the identification) were identified and their centres approximately located. After the computation of a 8-parameter transformation (rectification) between the two sets of coordinates, the position of the remaining targets in pixel coordinates was predicted and input to the template l.s.m. algorithm, to improve the accuracy of the localization. Note that if the transformation is not accurate enough and some predicted position may either fall between two targets or even on a different target; identification errors will therefore show up only in the bundle adjustment. This risk is obviously the higher the stronger the perspective deformation and therefore led to discard the last columns of targets in the Rollei images.

4.1 Template l.s.m.

The targets are nominally all the same and their background, apart from parasite reflections, is homogeneous: the conditions for automatic target location are therefore almost ideal. Rather than selecting a reference image (and therefore implicitly defining the target centres by applying some interest operator or computing some gravity centre), we preferred to prepare a synthetic template of the target and match it with each image patch drawn around the approximate target position. This makes the result also less dependent on the background characteristics (reflections and dirt on the negatives). To prepare the template, patches around the targets were extracted from images and g.v. profiles across the targets analyzed, to get a good match between the template's and the true g.v. distribution within the patches.

Due to the convergence of the side images, the image scale varies considerably and the perspective deformation of the targets is relevant. This, coupled with the relatively large size of the targets, which were not designed for this survey (target size on the P31 images varies from about 60 to 12 pixel), affects the automation level and the measurement accuracy of the l.s.m in two ways.

As far as automation level is concerned, the starting point of the matching is relatively close (within the target in most of the central four images) to the final position; since the point transfer includes scanner deformations for the Rollei images, the result was good, but to improve the succes rate of the matching four more initial position were selected around that computed.

Appropriate initial values for the shaping parameters of the l.s.m. were required: indeed, measuring the first side images it turned out clearly that the scale parameters were critical to ensure convergence of the matching, since at the initial iteration patch and template were too much different from each other. In addition, for the Rollei set, the perspective deformations were so high that roughly only in half image (the closest part of the object) we had sufficient correlation or unbiased estimation of the target centres.

As far as measurement accuracy is concerned, we considered at first the offset between the centre of the ellipse (the target on the image) with respect to the centre of the disk (true target

centre) according to the formula given in (Dold, 1996). The influence is larger for the P31 images, due to the larger image scale, even taking into account the stronger convergence of the Rollei images. A series of simulations with different convergence angles for the 100 mm lens showed that, in the farthest area of the panel, the offset is significant and, for the actual convergence angle used, is in the range 4-8 μm. Rather than apply the corrections, given the low correlations values obtained from the l.s.m., we decided to skip the last 6 columns from the side images.

As far as radiometric corrections are concerned, l.s.m. has been performed by equalizing mean and standard deviations of the g.v. for the template and the patch, before starting the iterations. To resample the patch, the geometric model we usually select is an affine transformation; a threshold of 0.75 was used for the correlation coefficient. In this case, after running the first block adjustment, it turned out that the accuracy we relied upon, as measured by σ_0 could not be achieved, for both set of images.

The measurement of the control points was performed interactively, assigning the initial position by a pointer on the screen. Here lower correlation values were reached, compare to the black targets, again because of the interference of the panel border (see figure 5).

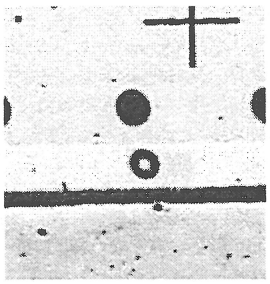

Figure 5 - A control point over the panel border.

5. BLOCK ADJUSTMENT

Several block adjustment have been computed using the program CALGE of DIIAR and the program Bingo, for both series of data. Based on the data snooping test, we found several small gross errors along the panel edges (on average 26 points per image). This is likely due to the fact that the targets are very close to the aluminium border of the panel: this shows always in one of the sides of the patch, preventing to reach good correlation or getting a biased estimate of the centre; the reliability of these points is therefore smaller than those inside the panel. On average there are 7.6 rays per point in both sets, because only approximately half image points were used in the convergent images.

Table 2 summarizes the results of the block adjustment: the first two rows compare the adjustment of the P31 and Rollei images with the program CALGE. The measurement accuracy, as estimated by sigma naught, is basically the same, thought the larger image scale yields a better variance propagation and therefore a theoretical accuracy within the specifications, while the Rollei just misses the goal. Figure 6 highlights the difference in 3D coordinates between the two sets. In any case, the empirical accuracy, estimated by the discrepancies over the 6 check points, is much better for the P31; actually, the discrepancies are significant at least for the coordinate Z.

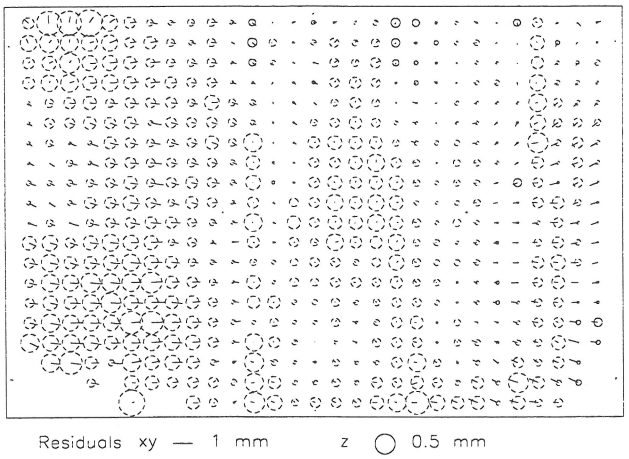

Figure 6 – Discrepancies of object coordinates between Rollei and P31.

					Tie points		Check points	
					Theoretical accuracy		Empirical accuracy	
Test	**n. of images**	**Check points**	σ_0 [μ]	$\frac{\sigma_0}{\text{pix. size}}$	σ_{xy} [mm]	σ_z [mm]	RMS_{xy} [mm]	RMS_z [mm]
P31	8	6+5	6.3	0.32	0.06	0.09	0.07	0.09
Rollei	8	6+5	6.0	0.30	0.14	0.16	0.37	0.49
P31 with self c.	8	-	5.8	0.29	0.06	0.08	-	-
Rollei with self c.	8	-	5.2	0.26	0.12	0.13	-	-
P31	4	6+5	7.4	0.37	0.15	0.30	0.22	0.49
Rollei	4	6+5	5.6	0.28	0.21	0.29	0.40	0.53

Table 2 - Bundle block adjustment results.

Since the results in absolute terms are not too satisfactory, we analyzed the residuals of the collinearity equations. In both sets there were characteristics patterns, thought not clearly systematic (see figure 7-a, b).
We may expect that from the Rollei set, since they may be interpreted as dependent on scanner distortions; this is less obvious for the P31. The pattern of the residuals, which looks as if made by different adjacent patches, may be also attributed to the scanner, which has a area sensor and therefore acquires the image in tiles.
Since CALGE does not include additional parameters, we also adjusted the observations with the program Bingo, to try to improve things at the adjustment level. As it can be seen from the 3rd and 4th row of Table 2, this improves sigma naught by less than 1 μm, with the Rollei getting the higher benefits.
The last two rows of Table 2 refer to the comparison of the two sets, using 4 images only, those approximately taken in normal mode. It is apparent that the RMS on the check point sharply increases also for the P31, meaning that the configuration is in fact rather weak, especially in elevation. Figure 8 show the differences in 3D coordinates of the two sets 8-4 images for Rollei camera, clearly larger for the P31 set, given the better base ratio of the Rollei network.

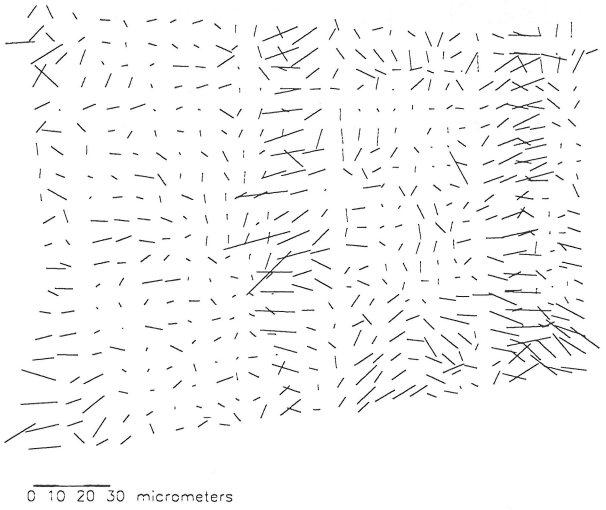

Figure 7 a – Residuals on a Rollei image.

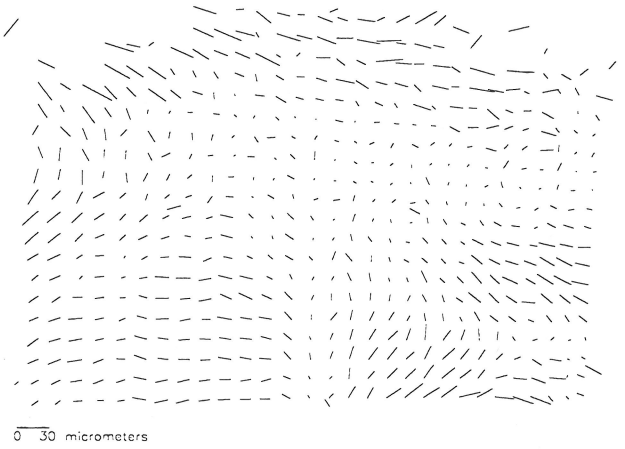

Figure 7 b – Residuals on a P31 image.

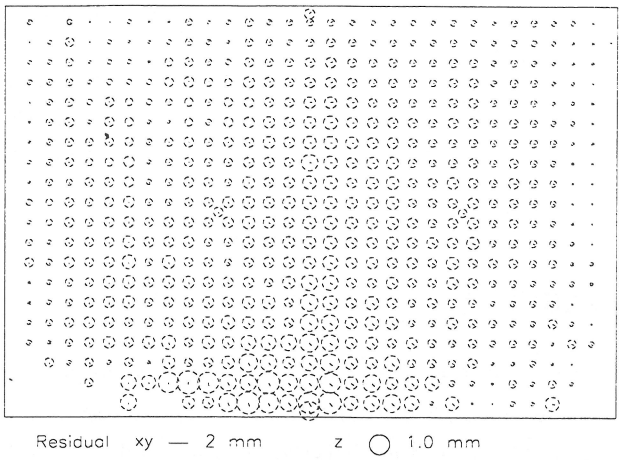

Figure 8 – Discrepancies of object coordinates between P31 8-images and P31 4-images.

6. CONCLUSIONS

Some questions about the pattern of the residuals remained unanswered. Sure, the high redundancy of the block made it possible to satisfy the accuracy requirements at least with one of the systems, but the goal would have been achieved also for the semimetric camera if a better measurement accuracy could have been obtained, since sigma naught is not very good in absolute terms. We may blame for that insufficient modelling the scanner deformations, but in the past (true, with a different DTP scanner) we got better results and we expected to do the same also this time.
And we hope that our next paper will be about images acquired by a digital camera.

References from Other Literature:

Dold, J., 1996. Influence of large targets on the results of photogrammetric bundle adjustment. In: Int. Archives of Photogrammetry and Remote Sensing, Vol. 31 Part 5, Vienna, 1996, pp. 119-123.
Forlani, G., Guzzetti F., Pinto L., 1996a. Surface reconstruction of CFER panels. In: Int. Archives of Photogrammetry and Remote Sensing, Vol. 31 Part 5, Vienna, 1996, pp. 209-214.
Forlani, G., Malinverni E.S., Pinto L., 1996b. A digital approach to the photogrammetric survey by reseau cameras. In: Reports on surveying and geodesy (in memory of A. Gubellini and G. Folloni), M.Unguendoli (ed), Nautilus, Bologna, Italy, pp. 355-366.